THERMAL INTERACTION MODEL

BETWEEN A FLUID FLOW AND A SOLID

D. E. Hryb† and M. B. Goldschmit‡

† *Center for Industrial Research, TenarisSiderca, Dr. Simini 250, Campana, Argentina.*
dhryb@tenaris.com
‡ *Sim&Tec S.A., Pueyrredón 2130, Buenos Aires, Argentina*
IMATEC, Engineering School, Universidad de Buenos Aires, Argentina
mgoldschmit@simytec.com

***Abstract*— A fluid dynamic – thermal coupled model was developed. This model takes into account the movement of solid contours and the thermal coupling between the different model domains (solid or liquid). The finite element method was employed to solve the conservation equations. The model gives the possibility that the different meshes are not connected; this generates a great flexibility in meshing and in geometry modification. The domains coupling algorithm could be validated using simple problems. Finally, the model developed was validated and applied successfully to the simulation of the fluid dynamic thermal behavior of hot dip galvanizing bath.**

***Keywords*— fluid dynamic, thermal, finite element method, coupled problem, continuous galvanizing.**

I. INTRODUCTION

Numerical fluid dynamics is nowadays a powerful and reliable tool for simulating different thermo-fluid dynamic processes. Hence, it permits to analyze different operative variables and geometrical configurations to investigate technological windows of different processes in metallurgical industry. In some cases, the industrial process involves moving solid contours like rotating cylinders or circulating strips. This solid contours exchange momentum and heat with the surrounding fluid. In this paper a fluid dynamic – thermal coupled numerical model was presented.

In section II the governing equations and the used hypothesis are presented. In section III the numerical scheme used to solve the equations and the coupling method are described. The model was validated with simple cases. In section IV The model was validated and applied to the galvanizing process. Finally, in section V the conclusions are presented.

II. GOVERNING EQUATIONS

A. Turbulent fluid dynamic – thermal model

In order to obtain the field of velocities, pressures and temperature in a turbulent incompressible fluid flow the equations of Navier Stokes and energy using the Boussinesq approximation are solved.

$$\nabla \cdot \mathbf{v} = 0 \tag{1}$$

$$\rho_f \frac{\partial \mathbf{v}}{\partial t} + \rho_f \mathbf{v}.\nabla \mathbf{v} - \nabla \cdot \left[\left(\mu + \mu^t\right)\left(\nabla \mathbf{v} + \nabla \mathbf{v}^T\right) \right] \ldots + \nabla P + \mathbf{F}_{bth} = \mathbf{0} \tag{2}$$

$$\rho_f Cp_f \left(\frac{\partial T}{\partial t} + \mathbf{v}.\nabla T_f \right) - \nabla \cdot \left[\left(\lambda_f + \lambda^t\right) \nabla T_f \right] + Q_f = 0 \tag{3}$$

$$\lambda^t = \frac{\mu^t \, Cp_f}{\mathrm{Pr}^t} \tag{4}$$

Where ρ_f is the fluid density, μ_f is the fluid laminar viscosity, μ^t is the turbulent viscosity, $\mathbf{v}$ is the time averaged velocity, p is the time averaged pressure, $\mathbf{F}_{bth} = \rho \mathbf{g} \beta_{th} \left(T - T^{ref}\right)$ is the buoyancy force, $\mathbf{g}$ is the acceleration due to gravity, β_{th} is the thermal expansion coefficient, Cp_f is the fluid specific heat, λ_f is the fluid thermal conductivity and Pr^t is the Prandtl turbulent number.

The mathematical description of the turbulent flows using mean quantities equations makes necessary the use of turbulence models to close the problem. For industrial problems modeling the mixl model or the k-ε model (Launder and Spalding 1974) are commonly used.

Due to the turbulence models cannot solve the flow in the zone near the solid contours, the wall functions method (Launder and Spalding 1974) is used. The finite element mesh is located at a wall distance Δ_{wall}. The friction velocity u^* is calculated solving the nonlinear equation

$$\frac{v_x}{u^*} = \frac{1}{\kappa} \ln\left(y^+ \, E\right) \qquad y^+ = \frac{\rho \, y \, u^*}{\mu} > 11.63 \tag{5}$$

And then, τ_w is applied in the corresponding fluid node.

$$\tau_w = \rho u^{*2} \tag{6}$$

In order to solve the thermal coupled problem the boundary layer temperature profile is considered to transfer the boundary condition as in the case of velocities. A similarity between the velocity profile and the temperature profile is assumed. The dimensionless temperature is obtained like

$$T^+ = \begin{cases} \Pr y^+ & y^+ < y_0^{\theta+} \\ \sigma^\theta \left[\frac{1}{k} \ln y^+ + P_T \right] & y^+ > y_0^{\theta+} \end{cases} \quad (7)$$

$$P_T = \frac{1}{\sigma^\theta} \left[\Pr y_0^{\theta+} - \frac{\sigma^\theta}{\kappa} \ln y_0^{\theta+} \right] \quad (8)$$

Then, knowing the solid wall temperature T_s a heat flow is applied $Q = h(T_s - T_f)$, where $h = \rho Cp u_* / T^+$ is the convective heat transfer coefficient.

B. Solid thermal model

In order to obtain the field of temperatures in the solid, the energy equation are solved.

$$\rho_s Cp_s \left(\frac{\partial T_s}{\partial t} + \mathbf{v}_s . \nabla T_s \right) - \nabla \cdot [\lambda_s \nabla T_s] + Q_s = 0 \quad (9)$$

Where ρ_s is the solid density, Cp_s is the solid specific heat transfer, T_s is the solid temperature, v_s is the solid velocity and λ_s is the solid thermal conductivity.

The term $\rho_s Cp_s \, \mathbf{v}.\nabla T_s$ allows modeling a moving solid seen from an eulerian point of view as to be rotating cylinders or plates moving in the direction of its axis as it is shown in figure 1.

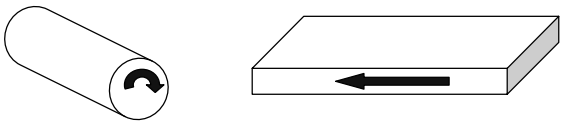

Figure 1 – moving solids

C. Coupling between fluid and solid model

In the first place, a connection between the solid and the fluid exists due to the tensions in the solid - fluid interface. These tensions are modeled through the wall functions, which were modified to consider the velocity of the moving solid contour, which is always tangent to the fluid - solid interface. The Eq. 8 takes the form

$$\frac{v_x - v_s}{u^*} = \frac{1}{\kappa} \ln(y^+ E) \quad (10)$$

where v_s is the solid contour velocity.

In the second place, a thermal connection between the fluid and the solid exists due to the heat exchange between both domains through the fluid - solid interface. This heat exchange is modeled by means of a Newton cooling law.

$$Q_f = h(T_s - T_f) \quad (11)$$

where h is the convective heat transfer coefficient, that is calculated by means of the thermal wall laws (Principe and Goldschmit, 1999) and T_s and T_f is respectively the solid temperature and the fluid temperature. For the solid we have

$$Q_s = -Q_f = h(T_f - T_s) \quad (12)$$

III. NUMERICAL SOLUTION

A. Finite element model

The Navier Stokes and scalar transport equations are solved using the streamline upwind Petrov Galerkin method (SUPG) and a Newton Raphson scheme. The pressure P is replaced in terms of the velocity in the equation (2) using the penalty of the incompressibility condition (Zienkiewicz and Taylor, 2000). The domain was approximated using 8 nodes linear isoparametric hexahedral elements.

B. Coupling scheme between different domains

Due to it is solved a reduced domain for the fluid, the meshes that approximate the different domains (solid and fluid domains) are not connected.

In order to connect the solid domain and the fluid dynamic model it is necessary to know, for each contour node of the fluid mesh, the solid contour velocity value in that point. Taking this velocity, it is obtain the equivalent tangential tension to apply in the contour fluid domain due to the relative movement between solid and fluid. For it, each fluid mesh contour node is projected on the solid contour (see Fig. 2).

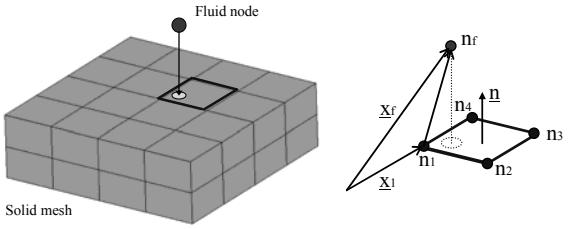

Figure 2 – projection scheme

This problem is limited to find the projection of a point on a plane. For each node of the fluid contour domain the following steps are made:

- a superficial element is taken from the solid domain and the distance between the fluid node and the plane that contain the superficial element is calculated.

$$dist = (\underline{x}_f - \underline{x}_1) \bullet \underline{n} \quad (13)$$

- If the *dist* value is negative or is not equal to Δ_{wall}, the element selected is rejected and another element is analyzed.
- If the *dist* value is equal to Δ_{wall}, the intersection point $\underline{x}_i$ is obtained

$$\underline{x}_i = \underline{x}_f - dist \cdot \underline{n} \tag{14}$$

- Then, the natural coordinates (r_i,s_i) are calculated, using the intersection point position xi and the four nodes coordinates $x_1,\ldots\ x_4$, solving the nonlinear equation system

$$\underbrace{\begin{bmatrix} h_1(r_i,s_i)\ldots\ h_4(r_i,s_i) & 0 & 0 \\ 0 & h_1(r_i,s_i)\ldots\ h_4(r_i,s_i) & 0 \\ 0 & 0 & h_1(r_i,s_i)\ldots\ h_4(r_i,s_i) \end{bmatrix}}_{\tilde{\mathbf{H}}} \begin{bmatrix} x_1 \\ \vdots \\ x_4 \\ y_1 \\ \vdots \\ y_4 \\ z_1 \\ \vdots \\ z_4 \end{bmatrix} = \begin{bmatrix} x_i \\ y_i \\ z_i \end{bmatrix} \tag{15}$$

- If r_i and s_i values are between [-1,1] the projection point is the correct. In the opposite case, the element selected is rejected and another surface element is analyzed.

Then, it is possible to obtain for each fluid contour node the corresponding solid velocity $\mathbf{v_s^f}$ according to the following equation

$$\tilde{\mathbf{H}}(r_i,s_i)\ \mathbf{V}_s^e = \mathbf{V}_s^f \tag{16}$$

In order to couple the fluid and solid thermal models is necessary to evaluate the heat exchange term (Eq. 11 and 12). This term discretized by finite element method takes the form

$$\mathbf{Q_f} = \left[h \int_{\Omega_e} \mathbf{H}^T\mathbf{H}\ d\Omega_e \right] \cdot \hat{\mathbf{T}}_\mathbf{s}^\mathbf{f} - \left[h \int_{\Omega_e} \mathbf{H}^T\mathbf{H}\ d\Omega_e \right] \cdot \hat{\mathbf{T}}_\mathbf{f} \tag{17}$$

Where $\hat{\mathbf{T}}_\mathbf{s}^\mathbf{f}$ are the solid temperature evaluated at the fluid contour nodes.

There are two possible solving schemes for the solid – fluid thermal coupling. One possibility is to solve the fluid and solid thermal equations in segregated manner, supposing known the solid temperature and solving the fluid temperature distribution. Then, the vector $\hat{\mathbf{T}}_\mathbf{s}^\mathbf{f}$ is obtained from

$$\tilde{\mathbf{H}}(r_i,s_i)\ \hat{\mathbf{T}}_s^e = \hat{\mathbf{T}}_s^f \tag{18}$$

In the same way, the solid temperature distribution is obtained supposing known the fluid temperature. This process is repeated until the convergence is achieved. This scheme introduces an iterative process to solve a linear problem, but it has the advantage to solve in each step a partial computational domain.

Another solving scheme, is to calculate simultaneously the fluid and solid temperature distributions solving an equation system of the form

$$\begin{bmatrix} \mathbf{K_{ff}} & \mathbf{K_{fs}} \\ \mathbf{K_{sf}} & \mathbf{K_{ss}} \end{bmatrix} \cdot \begin{bmatrix} \hat{\mathbf{T}}_\mathbf{f} \\ \hat{\mathbf{T}}_\mathbf{s} \end{bmatrix} = \begin{bmatrix} \mathbf{Q_f} \\ \mathbf{Q_s} \end{bmatrix} \tag{19}$$

Where the different matrix parts are as follow

$$\begin{aligned} \mathbf{Q}_\mathbf{f}^\mathbf{e} &= \underbrace{\left[h \iiint \mathbf{H}^T\mathbf{H}\ d\Omega_e \right] \cdot \tilde{\mathbf{H}}(r_i,s_i)}_{\mathbf{K_{fs}}} \cdot \hat{\mathbf{T}}_\mathbf{s}^\mathbf{e} - \underbrace{\left[h \iiint \mathbf{H}^T\mathbf{H}\ d\Omega_e \right]}_{\mathbf{K_{ff}}} \cdot \hat{\mathbf{T}}_\mathbf{f}^\mathbf{e} \\ \mathbf{Q}_\mathbf{f}^\mathbf{e} &= \underbrace{\left[h \iiint \mathbf{H}^T\mathbf{H}\ d\Omega_e \right] \cdot \tilde{\mathbf{H}}(r_i,s_i)}_{\mathbf{K_{sf}}} \cdot \hat{\mathbf{T}}_\mathbf{f}^\mathbf{e} - \underbrace{\left[h \iiint \mathbf{H}^T\mathbf{H}\ d\Omega_e \right]}_{\mathbf{K_{ss}}} \cdot \hat{\mathbf{T}}_\mathbf{s}^\mathbf{e} \end{aligned} \tag{20}$$

In this solving scheme the whole temperature distribution are obtained solving a bigger equation system, but with the advantage to avoid the iterative process.

The solving scheme is presented in figure 3, where in the first place the fluid dynamic problem is solved, then the coupled thermal problem is solved, and this process is repeated until the convergence is achieved for velocities and temperatures.

The convenience in the use of one either another scheme must be evaluated in each particular case based on the relative weight of the sizes of each involved domain and the possibility of including the temperature iterative scheme within an existing iterative process.

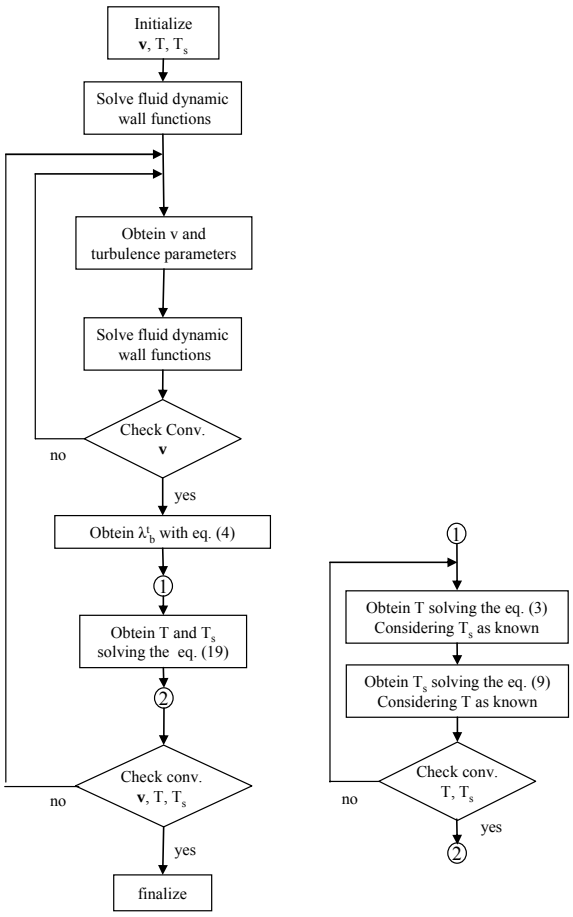

Figure 3 – solving scheme

C. Model verification

The fluid dynamic model and the thermal model developed was validated and used successfully in diverse industrial applications (Goldschmit et al, 1999, 2001, 2003, 2004).

In this work, only the validation of the coupling between the fluid dynamic thermal model and the moving solid thermal model is presented.

In the first place, the mapping algorithm was tested. For it, two different meshes with different densification were generated and it is applied a scalar distribution on the contour of a one of them. Then, using the mapping algorithm, the scalar is projected onto the other mesh contour. The meshes used are shown in Fig. 4.

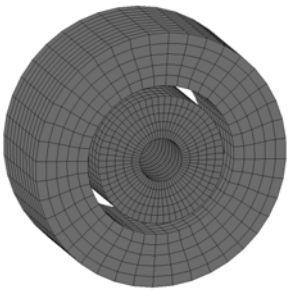

Figure 4 – meshes used to test the mapping algorithm

The scalar distribution is applied to the internal contour of the external ring, taking the form

$$A = sen^2(\theta) \tag{21}$$

In Fig. 5 the comparison between the analytical distribution and the projected distribution on the external contour of the internal ring is shown.

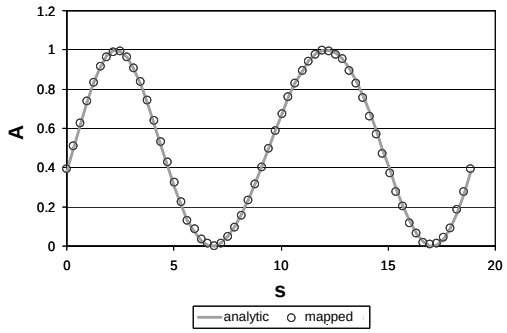

Figure 5 – scalar distribution comparison

In the second place, the solid energy equation convective term was tested. The strip circulation between two fluid blocks at rest was analyzed (see Fig. 6).

Figure 6 – circulation of strip

For the fluid domain the velocity was fixed to zero and the temperature to T_f. On the solid domain, the velocity was fixed to v_s and the inlet temperature was fixed to T_s^i. The two domains are meshed with different densification. In figure 7 the temperature distribution is showed for the whole domain.

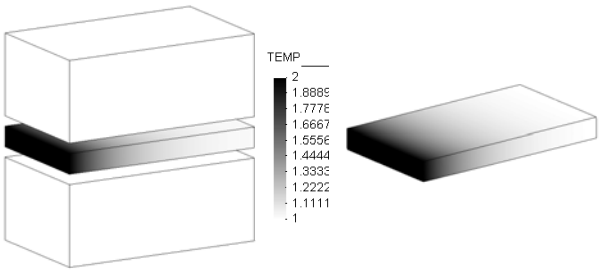

Figure 7 – temperature distribution

For this simple example it is possible to compare the strip temperature evolution in function of x (considering constant temperature in the thickness e) with the analytical result given by

$$T_s = (T_s^i - T_f)\exp\left(\frac{-2h\ x}{\rho ecpv_s}\right) + T_f \tag{22}$$

A good agreement between the analytical and the numerical strip temperature distribution is observed in figure 8.

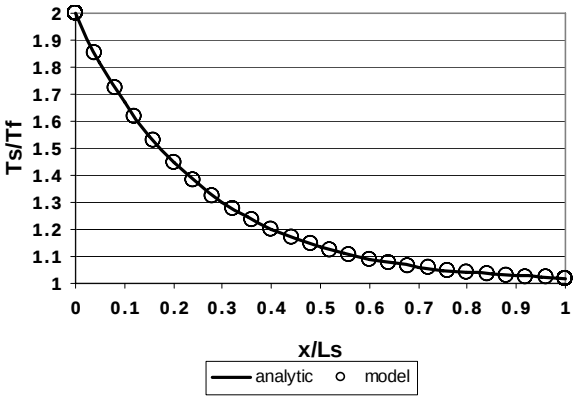

Figure 8 – strip temperature distribution

Finally, a problem of heat conduction was solved where the model domain is divided in three subdomains (see Fig 9) with independent meshes between them. The temperature was fixed at the top and the bottom surface of the whole domain. The coupling between the subdomains was achieved applying an equivalent heat transfer coefficient at the interfaces $h = \lambda/d$, where λ is the thermal conductivity coefficient and d is the gap between subdomains.

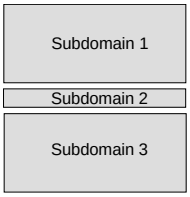

Figure 9 – subdomains

The dimensionless temperature distribution for the conduction problem is observed in Fig. 10

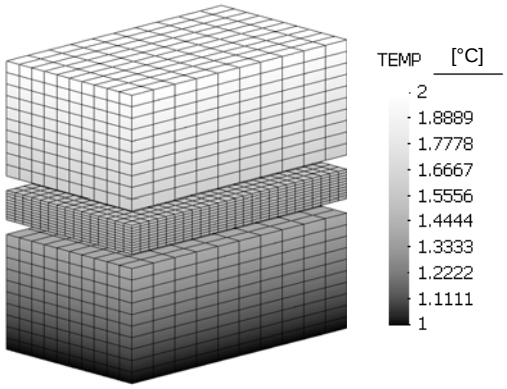

(a)

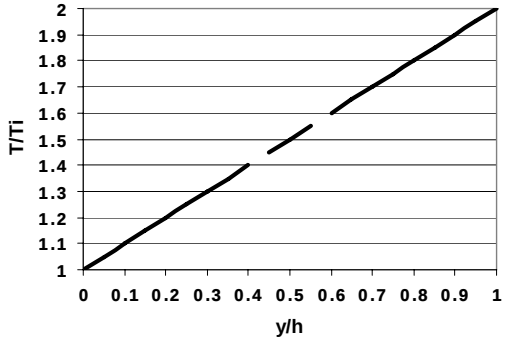

(b)

Figure 10 – dimensionless temperature distribution

It is observed that the obtained temperature distribution correspond to the analytical solution.

IV. INDUSTRIAL APPLICATION

The developed model was applied to hot dip galvanizing process. In the coating bath, the strip passes around a submerged roll and then exits the bath in a vertical direction. At the exit point, a set of gas knives (usually high pressure air), wipe off excess molten metal, leaving behind a closely controlled thickness of molten metal. In order to obtain a better understanding and optimize the galvanizing processes, it is necessary to know the fluid movement as well as the temperature distribution in the bath and the strip.

Gagne y Pare (1992) developed a water model to analyze the fluid dynamic behavior of galvanizing bath. Numerical models of this process has been published in Gagné y Gang (1998), Pare et al. (1995), Kato et al. (1995), Ajersch et al. (1998, 2001, 2002), Evans y Treadgold (1999), Baril et al. (2001), Mc Dermid et al. (2002). These numerical models don't solve the strip temperature distribution despising the bath – strip heat exchange.

A galvanizing pot scheme is showed in figure 11.

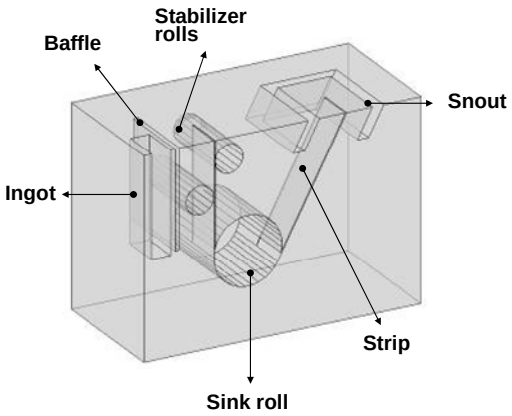

Figure 11 – pot scheme

Materials properties used to perform the simulations were considered constant and corresponding to those of melted zinc at a temperature of 460°C reference density ρ=6600 Kg/m3, laminar viscosity μ=0.004Pa.s, specific heat cp=512J/(Kg°C), thermal conductivity λ=60W/(m°C), and thermal expansion coefficient $\beta=1.666x10^{-4}\ °C^{-1}$.

A. Industrial fluid dynamic simulation

The fluid dynamic model was applied considering the boundary conditions showed in Figure 12. To take into account the turbulent effect the MIXL model with buoyancy correction was used (Rodi 1980).

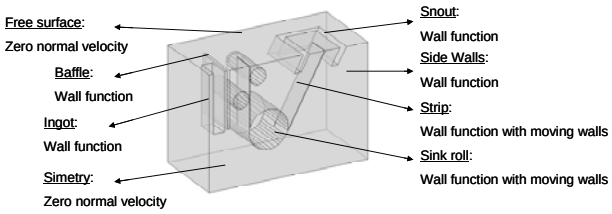

Figure 12 – fluid dynamic boundary conditions

The velocity module distribution divided by the strip velocity Vs is shown in the figure 13. It is observed that the higher velocities are concentrated near the strip and rolls.

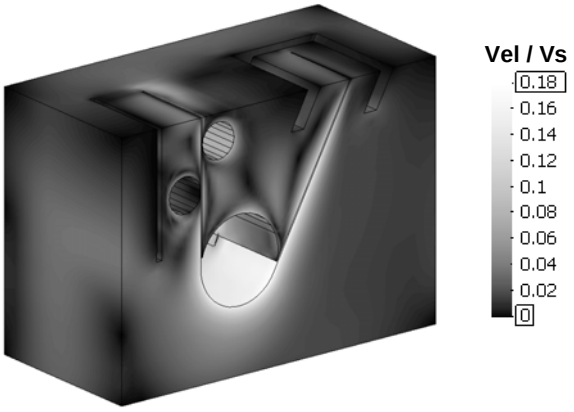

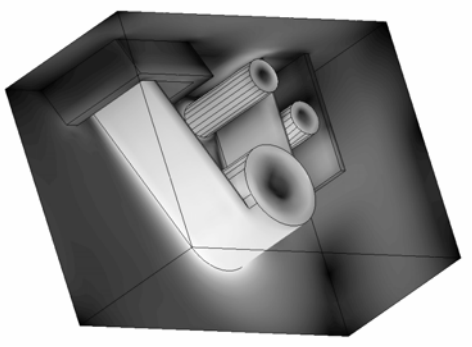

Figure 13 – velocity module distribution

B. Industrial thermal simulation

The thermal model was applied considering the boundary conditions showed in Fig. 14. To model the strip temperature evolution a 2D thermal model was used. The temperature variation through the strip thickness was not considered.

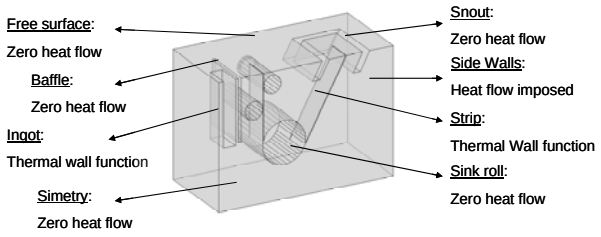

Figure 14 – thermal boundary conditions

In Figure 15, the bath temperature distribution divided by the strip entry temperature T^i_s is shown. It is observed that there is an increase of temperature in the zone of strip entry due to the important difference between the strip entry temperature of and the bath average temperature. In addition, due to the recirculation zones located above the sink roll, the dwell time of the fluid in this zone causes that the temperatures are greater to the average.

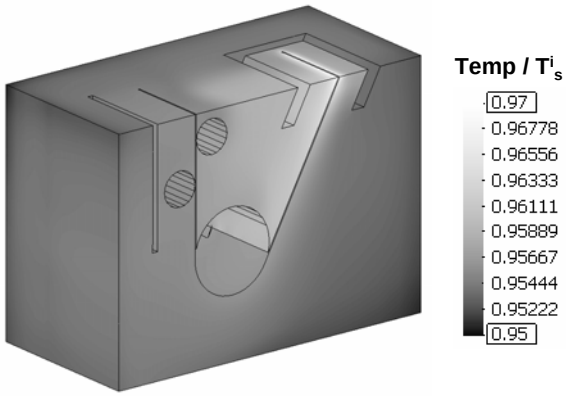

Figure 15 – bath temperature distribution

The strip temperature distribution is showed in figure 19. It is observed that the strip reaches quickly the bath temperature. There is a little temperature variation across the strip width due to the cold fluid that returns from lateral pot wall.

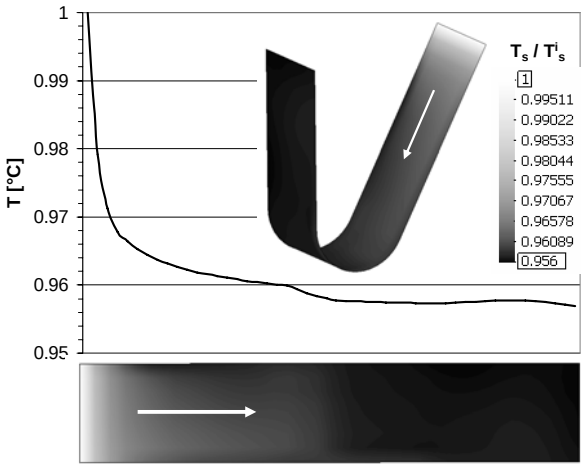

Figure 16 – strip temperature distribution

C. Industrial model validation

The validation of the fluid dynamic - thermal numerical model applied to the galvanizing process requires the measurement of velocities and temperatures in the bath. The velocity measurements present great experimental difficulties. The temperature measurements are simpler to make, not presenting great experimental difficulties, but it is necessary to have special care in calibrating the measurement device. In this report, temperature measurements are used to validate the numerical model developed.

In order to make the temperature measurements, one specific thermocouple with the following characteristics was made:

Thermopair: type K (Ni-Cr-Ni)
Bayonet: stainless steel 316
1" diameter
3 mm thickness
3 m length

Model validation was made with the measurement of the time evolution of the temperature at the control thermocouple point.

The time variations of heat resistance power and strip entry temperature are shown in the following figures.

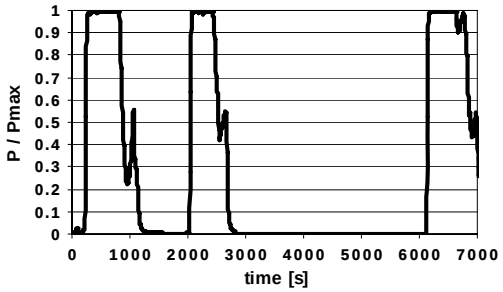

Figure 17 – heat resistance power

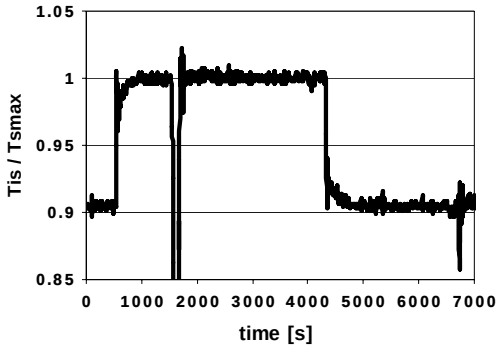

Figure 18 – strip entry temperature

The results of the stationary model were used as an initial condition for the transitory model. The strip entry temperature and fixed heat fluxes are used as boundary conditions. Figure 19 shows the comparison between the numerical results and experimental temperature measurements at the control thermocouple point.

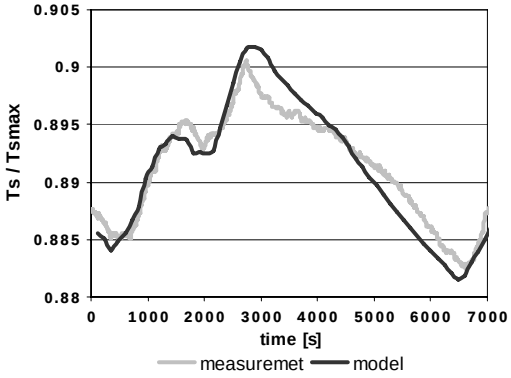

Figure 19 – Comparison between the numerical results and experimental temperature measurement at the control thermocouple point

The good agreement between the model and the measurements can be observed considering the precision necessary for an industrial model where there is a great amount of possible sources of uncertainty: thermocouple time response, heat losses, effective inductor heat power and strip entry temperature.

V. CONCLUSIONS

A fluid dynamic – thermal coupled model was developed. This model takes into account the movement of solid contours and the thermal coupling between the different model domains (solid or liquid). The model gives the possibility that the different meshes are not connected; this generates a great flexibility in meshing and in geometry modification. The domains coupling algorithm could be validated using simple problems. Finally, the model developed was validated and applied successfully to the hot dip galvanizing process.

REFERENCES

F. Ajersch et.al., "Validation studies of the numerical simulation of flow in the Bethlehem Steel, Burns Harbour galvanizing bath", Galvatech'98, Chiba, Japan, 642, 1998.

F. Ajersch et.al., "Numerical analysis of the effect of operating parameters on flow in a continuous galvanizing bath", Galvatech 2001, Brussels, Belgium, 511, 2001.

F. Ajersch, F. Ilinca and J.F. Héter, "Numerical analysis of the effect of temperature variation on flow in a continuous galvanizing bath", 44th MWSP Conference, vol. XL, 863, 2002.

E. Baril et.al., "Investigation of fluid flow in the snout of a continuous galvanizing bath using numerical modeling", Galvatech 2001, Brussels, Belgium, 435, 2001.

Bathe K. J., Finite Element Procedures, Prentice Hall, 1996.

Brooks and T.J.R. Hughes, "Streamline upwind Petrov-Galerkin formulations for convection dominated flows with particular emphasis on the incompressible Navier Stokes equations", Comp. Meth. in Applied Mech. and Engineering, 32, 199-259, (1982).

K.J. Evans and C.J. Treadgold, "Modeling and measurement of transient conditions in the galvanizing pot", 91st Galvanizer's Association Meeting, Jackson, MS, 131, 1999.

T.J.R. Hughes and A. Brooks, "A theoretical framework for Petrov-Galerkin methods with discontinuous weighting functions: application to the streamline-upwind procedure", Finite Elements in Fluids, 47-65, (1982).

M. Gagné and M. Gang, "Numerical modeling of fluid flow in continuous galvanizing baths", Galvatech'98, Chiba, Japan, 190, 1998.

M. Gagné, A. Pare and F. Ajersch, "Water modeling of continuous galvanizing baths", 84th Galvanizer's Association Meeting, Pittsburgh, PA, 147, 1992.

Kato et al, "Dross formation and flow phenomena in molten zinc bath", Galvatech'95, Chicago, IL, 801, 1995.

B.E. Launder and D.B. Spalding, "The numerical computation of turbulent flows", Comp. Meth. in Appl. Mech. And Engrg., 3, 269-289, 1974.

J.R. Mc Dermid, B.M. Maag and M. Gang, "Numerical modeling of ingot charching configurations at Pro-Tec CGL2", 94th Galvanizers Association Meeting, Dearborn, MI, 2002.

Pare, C. Binet and F. Ajersch, "Numerical simulation of 3-dimensional flow in a continuous strip galvanizing bath", Galvatech'95, Chicago, IL, 695, 1995.

R.J. Príncipe and M.B. Goldschmit, "Las condiciones de contorno sobre la pared en el modelado de flujo turbulento", VI Congreso Argentino de Mecánica Computacional, MECOM'99, Mendoza, 1999.

W. Rodi, "Turbulence models and their application in hydraulics. A state of the art review", Int. assoc. for Hydraulic Research, The Netherlans, 1980.

Zienkiewicz O.C. , and R.L. Taylor, The Finite Element Method.(5th. Edition), Mc Graw Hill, London (2000).